GENERAL LINEAR MODEL AND INFERENCE FOR NEAR INFRARED SPECTROSCOPY USING GLOBAL CONFIDENCE REGION ANALYSIS

Sungho Tak, Kwang-Eun Jang, Jinwook Jung, Jaeduck Jang, Jong Chul Ye

Bio-Imaging & Signal Processing Lab. Dept. of Bio and Brain Engineering
Korea Advanced Institute of Science and Technology (KAIST)
373-1 Guseong-dong Yuseong-gu, Daejon 305-701, Korea

ABSTRACT

Near infared spectroscopy (NIRS) is a non-invasive method to measure the brain activity as the changes of hemoglobin oxygenation through the intact skull. In this paper, we statistically analyze the NIRS data based on general linear model (GLM) and propose a new theory for making inference using Sun's tube formula. More specifically, we calculate the p-values as the excursion probability of an inhomogeneous Gaussian random field on a two dimensional representation manifold that are dependent on the structure of error covariance matrix and the interpolating kernels. These powerful tools for excursion probability allows us the super-resolution localization of the brain activation which is not possible using the conventional NIRS analysis.

Index Terms— near infrared spectroscopy, general linear model, statistical parametric mapping, excursion probability, inhomogeneous Gaussian random field, tube formula

1. INTRODUCTION

Near infrared spectroscopy (NIRS) is a non-invasive method to measure the brain activity by measuring the absorption changes of the near infrared light between 650 and 950 nm through the intact skull [1]. Specifically, the absorption spectra of oxy-hemoglobin ($\mathrm{HbO_2}$) and deoxy-hemoglobin (HbR) are distict in this region, so it is possible to determine the concentration changes of oxy- and deoxy-hemoglobin from diffusely scattered light measurement.

NIRS has many advantages over other neuroimaging modalities such as positron emission tomography (PET), functional magnetic resonance imaging (fMRI) or magnetoencephalography (MEG). One of the main advantages is the ability to measure a wide range of functional contrast such as oxy-hemoglobin, deoxy-hemoglobin, and total hemoglobin. Furthermore, high temporal resolution of NIRS allows us to study temporal behaviors of the hemodynamic response to neural activation and the origin of blood oxygenation level dependent signal (BOLD).

This research was supported in part by a Brain Neuroinformatics Research program by Korean Ministry of Commerce, Industry and Energy.

Recently, in NIRS domain, there have been many researches in statistical analysis of NIRS based on the general linear model (GLM) [2, 3]. GLM is a statistical linear model that explains data as a linear combination of an explanatory variable plus an error term. Because GLM measures the temporal variational pattern of signals rather than their absolute magnitude, GLM is robust to many cases even with a severe optical signal attenuation due to scattering or poor contact. Conventionally, Gaussian random field theory has been used for making the classical inference. The basic assumption for Gaussian random filed model is that the residuals after the GLM fitting are dense samples on lattice representations from an underlying continuous Gaussian random field due to the Gaussian kernel smoothing [4]. However, because the distance between each channel of NIRS is relatively far and the number of measurements is small, it is not reasonable to use Gaussian random field theory in making inference of NIRS data.

The main contribution of this paper is to propose a new theory of statistical inference which is appropriate to NIRS. Instead of calculating the excursion probability of the homogeneous Gaussian random filed, NIRS calculates the excursion probability of inhomogeneous Gaussian random field obtained by interpolating samples on sparsely and irregularity distributed optode locations. Even though excursion probability for inhomogeneous random filed is extremely difficult to calculate in general, the excursion probability for strikingly similar inhomogeneous random field model has been studied for the so-called global confidence region analysis of 3-D parametric shape estimation problem [5] using Sun's tube formula [6]. For example, the p-value for the one side t-test for oxy- or deoxy-hemoglobin concentration can be converted into the excursion probability of Gaussian random field on a two dimensional representation manifold that are dependent on the structure of covariance matrix and the interpolating kernels. These powerful tools for excursion probability allows the super-resolution localization of the brain activation which is not possible using the conventional methods.

2. MEASUREMENT MODEL FOR NIRS

The modified Beer-Lambert law (MBLL) which describes an optical attenuation in a highly scattering medium like biological tissue allows the transformation from raw optical density (OD) data to changes of chromophore concentrations. According to the MBLL, the change in $OD(\lambda, r, t)$ at the wavelength λ from the cerebral cortex position r at time t due to the N_c number of chromophore concentration changes $\{\Delta c^{(i)}(r,t)\}_{i=1}^{N_c}$ is described as

$$\triangle OD(\lambda, r, t) = -ln\left(\frac{I_F}{I_o}\right) = \sum_{i=1}^{N_c} a_i(\lambda) \triangle c^{(i)}(r,t) d(r) l(r), \tag{1}$$

where I_F denote the final measured optical intensity, I_o denotes the initial measured optical intensity, $a_i(\lambda)$ is the extinction coefficient of the i-th chromophore at the wavelength λ, $d(r)$ is the differential pathlength factor (DPF) at the position r, respectively. Assuming that oxy- and deoxy- hemoglobin are the major two choromophores, the noisy measured optical density changes are then described as follow:

$$\begin{bmatrix} \Delta OD(r,t;\lambda_1) \\ \Delta OD(r,t;\lambda_2) \end{bmatrix} = d(r) \cdot l(r) \cdot \begin{bmatrix} a_1(\lambda_1) & a_2(\lambda_1) \\ a_1(\lambda_2) & a_2(\lambda_2) \end{bmatrix} \cdot \begin{bmatrix} \Delta c_{HbO_2}(r,t) \\ \Delta c_{HbR}(r,t) \end{bmatrix} + \begin{bmatrix} w(r,t;\lambda_1) \\ w(r,t;\lambda_2) \end{bmatrix}, \tag{2}$$

where $\Delta c_{HbO_2}(r,t), \Delta c_{HbR}(r,t)$ denote the time-series of the chromophore changes for the oxy- and deoxy- hemoglobin; and $w(r,t;\lambda_1), w(r,t;\lambda_2)$ are the additive noise at the wavelength λ_1 and λ_2, respectively. Then, by multiplying the inverse matrix of the extinction coefficients with Eqn. (2), we have the noisy measurement of oxy- and deoxy- hemoglobin concentration changes:

$$\begin{bmatrix} y_{HbO_2}(r,t) \\ y_{HbR}(r,t) \end{bmatrix} = d(r)l(r) \begin{bmatrix} \Delta c_{HbO_2}(r,t) \\ \Delta c_{HbR}(r,t) \end{bmatrix} + \begin{bmatrix} \epsilon_{HbO_2}(r,t) \\ \epsilon_{HbR}(r,t) \end{bmatrix}, \tag{3}$$

where $\epsilon_{HbO_2}(r,t)$ and $\epsilon_{HbR}(r,t)$ are additive zero mean Gaussian noise for oxy- and deoxy- channel. In practice, it is impossible to measure the exact value of $d(r)$ and $l(r)$. This is because that the NIRS data acquisition is considerably affected by variety of measurement conditions such as the color of hair and the scalp depth, which make the position- and subject- dependent scattering effect. Non-uniform contact between optodes and a scalp might be another source of the variation of sensitivities of detectors. There are other experimental issues such as the subject's movement during the experiment. For these reasons, analyzing NIRS data with the absolute value of chromophore concentration is problematic.

3. GENERAL LINEAR MODEL FOR NIRS

In this section, we will show that GLM approach enables an accurate analysis for NIRS. Even though we mainly focus on the GLM for the oxy- hemoglobin concentration, exactly same approach can be applied for deoxy- hemoglobin concentration.

Let $\mathbf{y}_{HbO_2}^{(i)} \in \mathbb{R}^N$ and $\boldsymbol{\epsilon}_{HbO_2}^{(i)} \in \mathbb{R}^N$ denote the time series of the oxy- hemoglobin signal and noise at the i-th channel at the location r_i given by:

$$\mathbf{y}_{HbO_2}^{(i)} = \begin{bmatrix} y_{HbO_2}(r_i,t_1) & \cdots & y_{HbO_2}(r_i,t_N) \end{bmatrix}^T \tag{4}$$

$$\boldsymbol{\epsilon}_{HbO_2}^{(i)} = \begin{bmatrix} \epsilon_{HbO_2}(r_i,t_1) & \cdots & \epsilon_{HbO_2}(r_i,t_N) \end{bmatrix}^T \tag{5}$$

Then, corresponding GLM model is given by

$$\mathbf{y}_{HbO_2}^{(i)} = \mathbf{X}_{HbO_2} \boldsymbol{\beta}_{HbO_2}^{(i)} + \boldsymbol{\epsilon}_{HbO}^{(i)}, \tag{6}$$

where $\mathbf{X}_{HbO_2} \in \mathbb{R}^{N \times M}$ denotes the design matrices for oxy-hemoglobin, and $\boldsymbol{\beta}_{HbO_2}^{(i)} \in \mathbb{R}^{M \times 1}$ is the corresponding response signal strength at the i-th channel, respectively. By stacking the measurements from all K channels, we have

$$\mathbf{y}_{HbO_2} = \left(\mathbf{I}^{K \times K} \otimes \mathbf{X}_{HbO_2}\right) \boldsymbol{\beta}_{HbO_2} + \boldsymbol{\epsilon}_{HbO_2}, \tag{7}$$

where $\mathbf{I}^{K \times K}$ denotes the $K \times K$ identity matrix, $\otimes$ is the Kronecker product, and

$$\boldsymbol{\beta}_{HbO_2} = \begin{bmatrix} \boldsymbol{\beta}_{HbO_2}^{(1)} \\ \boldsymbol{\beta}_{HbO_2}^{(2)} \\ \vdots \\ \boldsymbol{\beta}_{HbO_2}^{(K)} \end{bmatrix}, \ \boldsymbol{\epsilon}_{HbO_2} = \begin{bmatrix} \boldsymbol{\epsilon}_{HbO_2}^{(1)} \\ \boldsymbol{\epsilon}_{HbO_2}^{(2)} \\ \vdots \\ \boldsymbol{\epsilon}_{HbO_2}^{(K)} \end{bmatrix} \in \mathbb{R}^{KM \times 1} \tag{8}$$

Using the property of the Kronecker product, the least square estimation of $\boldsymbol{\beta}_{HbO_2}$ is given by

$$\hat{\boldsymbol{\beta}}_{HbO_2} = \left(\mathbf{I}^{K \times K} \otimes \mathbf{X}_{HbO_2}^{\dagger}\right) \mathbf{y}_{HbO_2}, \tag{9}$$

where $\mathbf{X}_{HbO_2}^{\dagger} = \left(\mathbf{X}_{HbO_2}^T \mathbf{X}_{HbO_2}\right)^{-1} \mathbf{X}_{HbO_2}^T$ denotes the pseudo-inverse of $\mathbf{X}_{HbO_2}$. Under the null hypothesis, the mean value of the response signal strength is zero. Hence, the corresponding estimation error covariance matrix is given by

$$\begin{aligned} \mathbf{C}_{\hat{\boldsymbol{\beta}}_{HbO_2}} &= E\left[\hat{\boldsymbol{\beta}}_{HbO_2} \hat{\boldsymbol{\beta}}_{HbO_2}^H\right] \\ &= \left(\mathbf{I}^{K \times K} \otimes \mathbf{X}_{HbO_2}^{\dagger}\right) \mathbf{C}_{\boldsymbol{\epsilon}_{HbO_2}} \left(\mathbf{I}^{K \times K} \otimes \mathbf{X}_{HbO_2}^{\dagger T}\right) \end{aligned} \tag{10}$$

where $\mathbf{C}_{\boldsymbol{\epsilon}_{HbO_2}}$ denotes the error covariance matrix.

The main difficulty in analyzing NIRS is that there exists only small number of optode and the distance between the optode is relative large; hence, direct application of Gaussian random field model for interference is not appropriate for

NIRS. In order to study the correlation with fMRI, it is preferable that the NIRS data should be interpolated to the same resolution as fMRI. Specifically, the interpolated response signal strength at $r \in \Psi$ is given as follows:

$$\begin{aligned}\hat{\boldsymbol{\alpha}}_{HbO_2}(r) &= \sum_{i=1}^{K} \boldsymbol{\beta}_{HbO_2}^{(i)} b_i(r) \\ &= \left(\mathbf{b}(r)^T \otimes \mathbf{I}^{M\times M}\right) \hat{\boldsymbol{\beta}}_{HbO} \in \mathbb{R}^M, \quad (11)\end{aligned}$$

where $\mathbf{b}(r)$ denotes the interpolating kernel given by

$$\mathbf{b}(r) = \begin{bmatrix} b_1(r) & b_2(r) & \cdots & b_K(r) \end{bmatrix}^T \in \mathbb{R}^{K\times 1}. \quad (12)$$

Usually, the response of the signal of interest is calculated by inner product with a contrast vector:

$$\begin{aligned}X_{HbO_2}(r) &= \mathbf{c}^T \hat{\boldsymbol{\alpha}}_{HbO}(r) \\ &= \mathbf{c}^T \left(\mathbf{b}(r)^T \otimes \mathbf{I}^{M\times M}\right) \hat{\boldsymbol{\beta}}_{HbO_2} \\ &= \mathbf{B}(r)^T \hat{\boldsymbol{\beta}}_{HbO_2}. \quad (13)\end{aligned}$$

The corresponding error variance is

$$C_{X,HbO_2}(r) = \mathbf{B}(r)^T \mathbf{C}_{\hat{\boldsymbol{\beta}},HbO_2} \mathbf{B}(r) \quad (14)$$

Now, under the null hypothesis the response signal $X_{HbO_2}(r)$ is distributed as zero mean Gaussian distribution:

$$X_{HbO_2}(r) \sim \mathcal{N}\left(0, C_{X,HbO_2}(r)\right). \quad (15)$$

Hence, the corresponding t- statistics is given by

$$T_{HbO_2}(r) = \frac{\mathbf{B}(r)^T \hat{\boldsymbol{\beta}}_{HbO_2}}{\sqrt{\mathbf{B}(r)^T \mathbf{C}_{\hat{\boldsymbol{\beta}},HbO_2} \mathbf{B}(r)}}. \quad (16)$$

4. INFERENCE USING GLOBAL CONFIDENCE REGION ANALYSIS

Assuming that the interpolating kernel can fully describe the baseline signal between the optode locations, our goal is to calculate the p-value where the null hypothesis can be abandoned. This can be calculated as the excursion probability of the random field interpolated from the sparse measurement. Similar excursion probability has been extensively studied for the so-called global confidence region analysis for 3-D parametric shape estimation problem [5]. They showed that the resultant random field is inhomogeneous and its excursion statistics can be calculated using Sun's tube formula [6]. Hence, we follow the approach in [5] and calculate the p-values.

The p-value of the t- statistics to adandon null hypothesis is given by

$$\begin{aligned}p &= P\left\{\max_{r\in\Psi} T_{HbO_2}(r) \geq z\right\} \\ &= \frac{1}{2} P\left\{\max_{r\in\Psi} |T_{HbO_2}(r)|^2 \geq z^2\right\} \\ &= \frac{1}{2} P\left\{\max_{r\in\Psi} \mathbf{Z}^T \mathbf{P}_{HbO_2}(r) \mathbf{Z} \geq z^2\right\}. \quad (17)\end{aligned}$$

where $\mathbf{Z} \sim \mathcal{N}\left(\mathbf{O}, \mathbf{I}^{KM\times KM}\right)$ denotes the zero-mean independent Gaussian random vector and

$$\mathbf{P}_{HbO_2}(r) \triangleq \mathbf{C}_{\hat{\boldsymbol{\beta}},HbO_2}^{1/2} \mathbf{B}(r) C_{X,HbO_2}(r)^{-1} \mathbf{B}^T(r) \mathbf{C}_{\hat{\boldsymbol{\beta}},HbO_2}^{1/2} \quad (18)$$

Using Eqs. (13) and (14), we have

$$\mathbf{P}_{HbO_2}(r) = \mathbf{u}_{HbO_2}(r) \mathbf{u}_{HbO_2}(r)^T, \quad (19)$$

where the unit vector $\mathbf{u}_{HbO_2}$ is given by

$$\mathbf{u}_{HbO_2} = \frac{\mathbf{C}_{\hat{\boldsymbol{\beta}},HbO_2}^{1/2} \mathbf{B}(r)}{\sqrt{\mathbf{B}(r)^T \mathbf{C}_{\hat{\boldsymbol{\beta}},HbO_2} \mathbf{B}(r)}}. \quad (20)$$

Ye et al [5] derived the two approximation for the probability in Eq. (17). First, the incomplete gamma bound comes as following:

$$\begin{aligned}P\left\{\max_{r\in\Psi} \mathbf{Z}^T \mathbf{P}_{HbO}(r) \mathbf{Z} \geq z^2\right\} &\geq P\left\{\max_{r\in\Psi} \mathbf{Z}^T \mathbf{Z} \geq z^2\right\} \\ &= 1 - \Gamma\left(\frac{KM}{2}, \frac{z^2}{2}\right) \quad (21)\end{aligned}$$

For small number of channel (i.e. K is smaller), then incomplete gamma bound is quite tight [5]. However, for large number of channels, we may need more accurate approximation. This can be calculated using Sun's tube formula [6]. Now, let us define an inhomogeneous Gaussian random field

$$X_{HbO_2}(r) = \mathbf{u}_{HbO_2}(r)^H \mathbf{Z}. \quad (22)$$

Now, a more compact representation for $X(r)$ is in terms of the two-dimensional representation manifold [5]:

$$\mathcal{U} \triangleq \{\mathbf{u}_{HbO_2}(r), r \in \Psi\} \quad \subset \mathbb{R}^{KM}. \quad (23)$$

While the functional representation $\mathbf{u}(\cdot)$ of a manifold is nonunique, there are several quantities that are intrinsically related $\mathcal{U}$. One of them is the 2×2 *metric tensor matrix*:

$$\mathbf{R}(r) \triangleq E[\nabla X_{HbO_2}(r) \nabla^T X_{HbO_2}(r)]. \quad (24)$$

Then, finally we derive the following approximation:

$$P\left\{\max_{r\in\Psi} \mathbf{Z}^T \mathbf{P}_{HbO_2}(r) \mathbf{Z} \geq z^2\right\} \simeq \kappa_0 \psi_0(z), \quad (25)$$

where

$$\kappa_0 = |\mathcal{U}| = \int_\Psi \sqrt{|\det(\mathbf{R}(r))|} dr \quad (26)$$

and

$$\psi_0(z) = \frac{\Gamma\left(\frac{3}{2}\right)}{2\pi^{3/2}} \left(1 - \Gamma\left(\frac{3}{2}, \frac{z^2}{2}\right)\right). \quad (27)$$

The formula for p-value for the case of HbR can be derived in a same manner. We now summarize the results in the following:

Theorem 4.1 *The p-value for the one side t- test for* $\mathrm{HbO}_2/\mathrm{HbR}$ *is lower bounded by*

$$p \geq \frac{1}{2}\left(1-\Gamma\left(\frac{KM}{2},\frac{z^2}{2}\right)\right). \quad (28)$$

Furthermore, the tube formula approximation of the p-value is given by

$$p \simeq \frac{\kappa_0\Gamma\left(\frac{3}{2}\right)}{4\pi^{3/2}}\left(1-\Gamma\left(\frac{3}{2},\frac{z^2}{2}\right)\right) \quad (29)$$

where κ *is given by Eq.* (26)*.*

5. EXPERIMENTAL RESULTS

To evaluate the practical usefulness of proposed methods, we applied our new statistical analysis framework to right finger tapping experiment data. The primary motor cortex is the target region of right finger tapping task. Experimental data were simultaneously acquired using a NIRS and fMRI system. Specifically, a NIRS system has 8 laser diodes and 4 detectors (Oxymon MK III, Artinis, Netherlands). In this system, two continuous wave light (781nm, 856nm) were emitted at each source fiber. The distance between source and detector was 3.5cm. MR images covering the whole brain were acquired with the echo planar imaging (EPI) sequence using a 3.0T MRI system (ISOL, Korea). In right finger tapping experiment, the subject were instructed to perform a finger flexion and extension repeatedly during task period. Figures 1 show the GLM results from right finger tapping task. The activation map using fOSA [3] with Gaussian random field model is shown in Fig. 1(a). Note that fOSA cannot analyze the interpolated random field, so the estimated activated area is very rough. Our t-maps of $\Delta\mathrm{HbO}_2$ over the threshold obtained using incomplete gamma bound and Sun's tube formula are shown in Figs. 1(b) and (c), respectively. Note that our activation pattern of $\Delta\mathrm{HbO}_2$ is fairly consistent with that of BOLD signal, as shown in Figs. 1(d). The incomplete gamma bound gives very optimistic estimate of the activated area, whereas the tube formula tells us that the more areas are activated by the finger tapping. Both of the results exhibits excellent correlation with the fMRI result. Furthermore, compared to fOSA results in Fig. 1(a), our method allows super-resolution localization.

6. CONCLUSION

We proposed a new theory of statistical inference which is optimal for NIRS. Instead of calculating the excursion probability of the homogeneous Gaussian random field by smoothing samples on dense lattice, we calculated the p-value as the excursion probability which comes from the random field that are interpolated from the sparse measurement. Experimental results from the right finger tapping task showed that the proposed method can localize the activation of primary motor cortex very accurately.

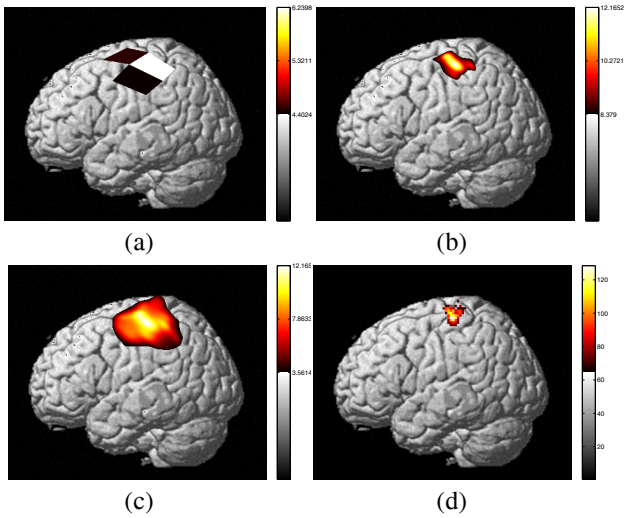

Fig. 1. Activation area using (a) fOSA [3], and (b) incomplete Gamma bound, (c) tube formula, and (d) fMRI. p-value: 0.01.

7. REFERENCES

[1] A. Villringer and U. Dirnafl, "Coupling of brain activity and cerebral blood flow: basis of functional neuroimaging," *Cerebrovasc. Brain Metab. Rev.*, vol. 7, pp. 240–276, 1995.

[2] M. M. Plichta, S. Heinzel, A. C. Ehlis, P. Pauli, and A. J. Fallgatter, "Model-based analysis of rapid event-related functional near-infrared spectroscopy (nirs) data: A parametric validation study," *NeuroImage*, vol. 35, pp. 625–634, April 2007.

[3] P. H. Koh, D. E. Glaser, G. Flandin, S. Kiebel, B. Butterworth, A. Maki, D. T. Delpy, and C. E. Elwell, "Functional optical signal analysis: a software tool for near-infrared spectroscopy data processing incorporating statistical parametric mapping," *J. Biomed. Opt.*, vol. 12, pp. 1–13, November/December 2007.

[4] K. J. Friston, J. Ashburner, S. Kiebel, T. Nichols, and W. Penny, "Statistical parametric mapping: The analysis of functional brain images," *Academic Press*, December 2006.

[5] J. C. Ye, P. Moulin, and Y. Bresler, "Asymptotic global confidence regions for 3-d parametric shape estimation in inverse problems," *IEEE Trans. Image Process.*, vol. 15, pp. 2904–2919, October 2006.

[6] J. Sun, "Tail probabilities of the maxima of gaussian random fields," *Ann. Prob.*, vol. 21, pp. 34–71, January 1993.